

Robust Driving Path Detection in Urban and Highway Scenarios Using a Laser Scanner and Online Occupancy Grids

Thorsten Weiss, Bruno Schiele and Klaus Dietmayer

Abstract—Many driver assistant and safety systems depend on an accurate environmental model containing the positions of stationary objects, the states of dynamic objects and information about valid driving corridors. Therefore, a robust differentiation between moving and stationary objects is required. This is challenging for laser scanners, because these sensors are not able to measure the velocity of objects directly. Therefore, an advanced occupancy grid approach, the online map, is introduced, which enables the robust separation of moving and stationary objects. The online map is used for the robust detection of the road boundaries for the determination of driving corridors in urban and highway scenarios. An algorithm for the detection of arbitrary moving objects using the online map is proposed.

I. INTRODUCTION

Many common and future driver assistant and safety systems rely on the data of environmental sensors. Sensor systems such as radar, video or laser scanners provide information about stationary and moving objects in the field of view. Many algorithms and applications such as situation assessment as well as cooperative systems benefit from a detailed environmental model containing the positions of stationary objects and also the dynamic states of moving objects. In this work a laser scanner with a large horizontal opening angle, which is important in urban areas, such as intersections or acute bends, is used.

As laser scanners are not able to measure the velocity of objects directly, common object tracking and classification approaches are used to determine the dynamic states of moving objects [1], [2]. There are model assumptions, such as the dimension or the shape of tracked and classified objects. That's why it is hard to separate arbitrary moving objects and arbitrary stationary objects from each other in general. Especially the shape of stationary objects, such as bushes, house walls and all other objects, which can be found in the environment of the vehicle, is strongly varying. That's why a grid based method is chosen in this work to separate moving and arbitrary stationary objects.

Therefore, a special form of occupancy grids based on a binary bayes filter is introduced in section III. Within this approach, the region around the vehicle is partitioned into grid cells. For each grid cell a likelihood of occupancy is

Thorsten Weiss is with the Department Measurement, Control and Microtechnology, University of Ulm, D-89081 Ulm, Germany thorsten.weiss@uni-ulm.de

Bruno Schiele is a diploma students at the Department Measurement, Control and Microtechnology

Klaus Dietmayer is professor at the Department Measurement, Control and Microtechnology, University of Ulm, D-89081 Ulm, Germany klaus.dietmayer@uni-ulm.de

calculated in consideration of the distance measurements of the laser scanner. We denote this to the *online map*.

Thrun et. al. described a related algorithm for mapping approaches [3], [4] as well as within the DARPA grand challenge [5]. The approach was extended and modified in order to use it in the field of real-time driver assistant systems in urban and highway scenarios.

With the help of the online map road boundaries are detected and a driving corridor is determined using a new approach, which is introduced in section IV. Furthermore, the robust detection of arbitrary moving objects from the online map, without any common multi object tracking algorithms, is proposed in section V. One significant advantage of this approach is the fact, that no model assumptions are required to separate moving and stationary objects.

II. SENSOR SETUP

The multilayer laser scanners ALASCA XT (Automotive LaserScanner) of IBEO Automobile Sensor GmbH acquire distance profiles of the vehicle's environment of up to 270° horizontal field of view [6]. The angular resolution is up to 0.125° and the scan frequency is chosen to 10 Hz in this work. The laser scanners use four scan planes with a vertical opening angle of 3.2° . The scanners are integrated at the front bumper of our testing vehicles as shown in Fig. 1.



Fig. 1. The laser scanners IBEO ALASCA XT are integrated at the front bumper of the testing vehicles.

III. ONLINE OCCUPANCY GRID MAPPING

In this section, a real time algorithm for the generation of advanced occupancy grids using distance measurements of the laser scanner is proposed. The algorithm is related to the approach *Occupancy Grid Mapping* described in detail by Thrun et. al. in [3]. Modifications and extensions for the use in real-time driver assistant applications are introduced.

The basic idea of the algorithm is the partition of a certain region around the vehicle to grid cells. The likelihood of occupancy of grid cells are updated in consideration of the actual distance measurements of the laser scanner using a

binary bayes filter. Thus, each cell contains the history of the previous laser scans.

In the following sections m_i denotes the i -th cell. The region is partitioned around the host vehicle into grid cells. All grid cells m_i form the occupancy grid $m = \{m_i\}$, which is denoted in this work to the *online map*. $p(m_i)$ is denoted to the occupancy likelihood. The likelihood $p(m_i) = 0$ stands for a free cell m_i and $p(m_i) = 1$ stands for an occupied cell m_i [3].

A. Advanced forward inverse sensor model

In order to combine the actual measurement and the existing online map, a separate grid with the same dimension as the online map is defined. The grid is denoted to *measurement grid* in this paper. The measurement grid contains the occupancy likelihoods $p(m_j|z_t)$ in consideration of the actual distance measurements z_t at time t .

1) *Initialization of the measurement grid:* All cells m_j of the measurement grid are set to $p(m_j) = 0.5$, before any distance measurements are registered, because it is not known, whether cells are occupied or not.

2) *Registration of distance measurements in the measurement grid:* The vehicle’s pose relative to the online map is known precisely. Each measurement point is transformed to the coordinate system of the online map. Thus, each measurement point is assigned to a certain cell in the measurement grid. There are often more than one distance measurements in some cells, as the dimension of the grid cell is chosen to 20 cm in this work. For each measurement point in a cell m_j , the value 0.05 is added to the cell likelihood $p(m_j)$. The value 0.05 is a heuristic parameter determined from extensive tests.

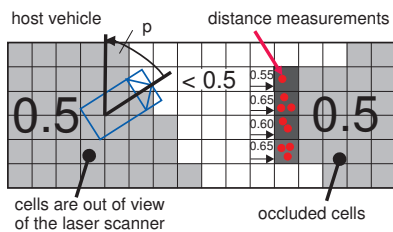


Fig. 2. Cells, which are out of view of the laser scanner or which are occluded ($p(m_j) = 0.5$) are painted gray. Occupied cells ($p(m_j) > 0.5$) are painted darker. Free cells ($p(m_j) < 0.5$) are painted brighter.

3) *Free regions in the measurement grid:* There is also information about free space in the distance profile of the laser scanner. If the laser scanner detects an object, the line between the laser scanner and the object seems to be free. However, if the laser scanner detects an object, there is no information about the region behind the object. Consequently, these regions must be neglected and the cells keep their initial likelihood of occupancy $p(m_o) = 0.5$ (see Fig. 2 and 3).

The discrete angle steps of the laser scanner are known [6]. If the laser scanner does not detect an object at certain angle steps, regions in that line also seem to be free.

Nevertheless, in far distances there may be small objects such as small posts, which are not detected by a laser beam of the actual scan. Therefore, the grid cells, which are situated along a beam are not all set simply to zero, but the cells are set to a value, which depends on the radial distance of the laser beam.

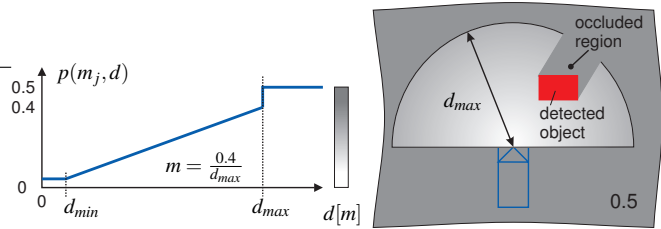


Fig. 3. The likelihoods of cells in the measurement grid depends on the radial distance to the laser scanner.

Therefore, a linear function is used. For a grid cell m_j , which is situated at a radial distance of d , the likelihood of the cell is:

$$p(m_j, d) = \begin{cases} 0.4 \cdot \frac{d - d_{min}}{d_{max} - d_{min}} & \text{for } 0 \leq d \leq d_{max} \\ 0.5 & \text{for } d > d_{max} \end{cases} \quad (1)$$

d_{max} is a design parameter and it is chosen with respect to the requirements of the application. In our application it is chosen to $d_{max} = 50$ m, although the field of view of the laser scanner is up to 200 m. d_{min} is the minimal radial distance and it chosen to 0.1 m. Fig. 3 illustrates the registration of free regions in the measurement grid.

Fig. 4 shows two exemplary measurement grids from real laser scanner data for an urban and a highway scenario.

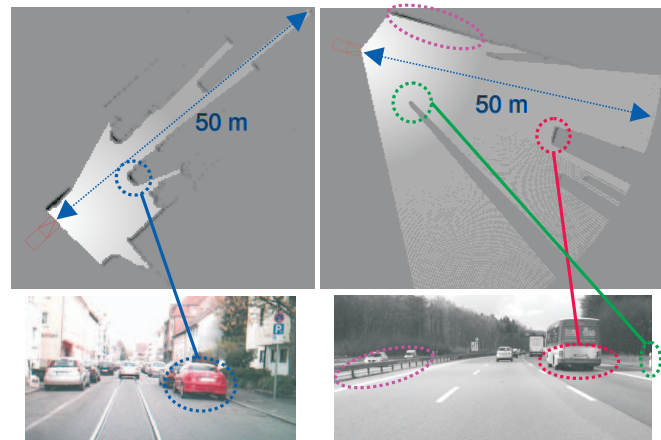


Fig. 4. Left: Measurement grid of an urban scenario. Right: Measurement grid of a highway scenario. The reference video images show the scenarios.

B. Update of the online map

The existing online map and the measurement grid are combined using a binary bayes filter, which addresses estimation problems with binary state, that does not change over time. In this approach the occupancy of a grid cell, which

remains at the same position and does not change during sensing, is estimated [3].

Each cell i of the online map contains the probability of occupancy in consideration of all preceding measurements $p(m_i|z_1, \dots, z_{t-1})$. The likelihoods of the cells of the actual online map $p(m_i|z_1, \dots, z_t)$ are determined from the existing online map and the actual measurement grid $p(m_i|z_t)$ using Bayes Theorem:

$$p(m_i|z_1, \dots, z_t) = \frac{p(z_t|z_1, \dots, z_{t-1}, m_i) \cdot p(m_i|z_1, \dots, z_{t-1})}{p(z_t|z_1, \dots, z_{t-1})} \quad (2)$$

The measurement in a cell i does not depend on the preceding measurements: $p(z_t|z_1, \dots, z_{t-1}, m_i) = p(z_t|m_i)$. After applying Bayes Theorem $p(A|B) = \frac{p(B|A) \cdot p(A)}{p(B)}$ to $p(z_t|m_i)$, equation 2 is then:

$$p(m_i|z_1, \dots, z_t) = \frac{p(m_i|z_t) \cdot p(z_t) \cdot p(m_i|z_1, \dots, z_{t-1})}{p(m_i) \cdot p(z_t|z_1, \dots, z_{t-1})} \quad (3)$$

Equation 3 gives the probability for an occupied cell i . Analogous, equation 4 gives the probability for a free cell i :

$$p(\bar{m}_i|z_1, \dots, z_t) = \frac{p(\bar{m}_i|z_t) \cdot p(z_t) \cdot p(\bar{m}_i|z_1, \dots, z_{t-1})}{p(\bar{m}_i) \cdot p(z_t|z_1, \dots, z_{t-1})} \quad (4)$$

Equation 3 is divided by equation 4:

$$\frac{p(m_i|z_1, \dots, z_t)}{p(\bar{m}_i|z_1, \dots, z_t)} = \frac{p(m_i|z_t)}{p(\bar{m}_i|z_t)} \cdot \frac{p(\bar{m}_i)}{p(m_i)} \cdot \frac{p(m_i|z_1, \dots, z_{t-1})}{p(\bar{m}_i|z_1, \dots, z_{t-1})} \quad (5)$$

With respect to $p(\bar{A}) = 1 - p(A)$ and $p(\bar{A}|B) = 1 - p(A|B)$ equation 5 is then:

$$\frac{p(m_i|z_1, \dots, z_t)}{1 - p(m_i|z_1, \dots, z_t)} = \frac{p(m_i|z_t)}{1 - p(m_i|z_t)} \cdot \frac{1 - p(m_i)}{p(m_i)} \cdot \frac{p(m_i|z_1, \dots, z_{t-1})}{1 - p(m_i|z_1, \dots, z_{t-1})} \quad (6)$$

For all cells in the measurement grid without any measurement points or free space (out of view or occluded cells), we set $p(m_i) = 0.5$. Equation 6 is then:

$$\frac{p(m_i|z_1, \dots, z_t)}{1 - p(m_i|z_1, \dots, z_t)} = \frac{p(m_i|z_t)}{1 - p(m_i|z_t)} \cdot \frac{p(m_i|z_1, \dots, z_{t-1})}{1 - p(m_i|z_1, \dots, z_{t-1})} \quad (7)$$

Finally, the *odds ratio* of a cell i in the online map is calculated:

$$p(m_i|z_1, \dots, z_t) = \frac{S}{1 + S} \quad (8)$$

$$S = \frac{p(m_i|z_t)}{1 - p(m_i|z_t)} \cdot \frac{p(m_i|z_1, \dots, z_{t-1})}{1 - p(m_i|z_1, \dots, z_{t-1})} \quad (9)$$

In [3] a *log odds ratio* form of the likelihood is proposed, as the bayes filter for updating beliefs in log odds representation is computational elegant, as *log odds ratio* assumes values from $-\infty$ to ∞ . It avoids truncation problems that arises for probabilities close to 0 or 1 [3].

However, we chose the formulation in equation 8 for two reasons. The calculation of the logarithm is computational expensive even if look-up tables are used. Furthermore, the range of the log odds ratio is $-\infty$ to ∞ , which is hard to

implement. The range of the odds form in equation 8 is 0..1, which is easier to handle using a 32 bit digit in a DSP or computer, for instance. The problematic truncation problem close to 0 and 1 is considered for by a simple procedure:

```

for all online map cells i do
  if probability of cell i in measurement grid is
  unequal to 0.5 then
    calculate odds ratio (equation 8)
  if  $p(m_i|z_1, \dots, z_t)$  is greater than  $1 - \epsilon$  then
    set  $p(m_i|z_1, \dots, z_t) = 1 - \epsilon$ 
  if  $p(m_i|z_1, \dots, z_t)$  is less than  $\epsilon$  then
    set  $p(m_i|z_1, \dots, z_t) = \epsilon$ 
  
```

ϵ may be set to 0.00001 for *float* variables, for instance. Extensive tests have shown, that this approach leads to very satisfying results. The performance of applications based on the online map using the odds ratios is the same as if log odds ratios are used, but with a significant lower computation time. the computation time for an update step is 25 ms (Pentium IV-M, 1,6 GHz). Fig. 5 shows an exemplary urban scenario, the actual measurement grid and the online map.

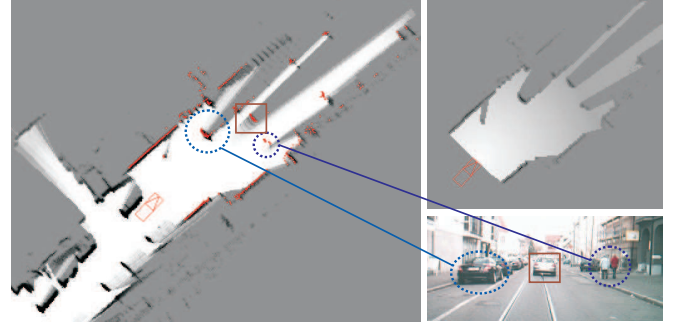


Fig. 5. The red points in the online map are the distance measurements of the actual laser scan. The measurement grid of the actual distance profile and a reference video image are shown. The two pedestrians are walking on a free region, which allows for the detection of these slowly moving objects.

C. Vehicle movement

1) *Movement Estimation*: The movement of the vehicle is determined using the integrated serial sensors. The translation and change of orientation is determined from the yaw rate, steering angle and wheel speed encoders. In standard situations (no sliding or wheelspin), the accuracy of the ego motion estimation is satisfying for this approach.

2) *Vehicle Movement in the Online Map*: In the first step the translation Δx_v^m , Δy_v^m and the change of the orientation $\Delta \psi_v^m$ of the vehicle are determined using the ego motion estimation algorithms. The translation and orientation of the vehicle are transformed to the coordinate system of the online map.

The position of the vehicle in the map is not only given by the center of the cell, where the origin of the vehicle's coordinate system is situated, but by an accurate position

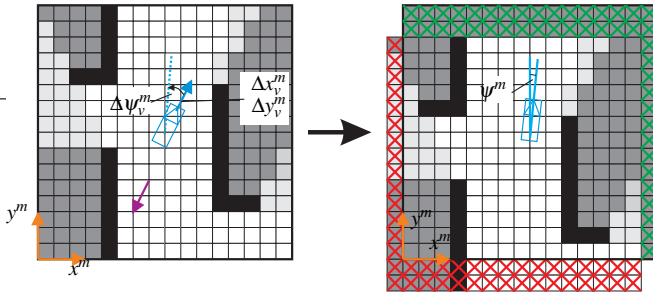


Fig. 6. Cells are added (green crosses) and opposite cells are removed (red crosses) dependent on the vehicle’s movement. The vehicle is rotated relative to the map coordinate system by the angle $\Delta\psi_v^m$. The blue box represents the host vehicle.

in the map coordinate system. Thus, the position of the vehicle inside the cell is known precisely. The number of columns and rows, which were passed by the vehicle, are calculated. The dimension of the online map is constant, which leads to a constant number of rows and columns. In this approach the vehicle moves virtually over the map, but only a quadratic region (the online map) is held in the memory of the computer. Thus, the map is shifted under the vehicle. Consequently, cells in driving direction are added and cells at the opposite site are removed as illustrated in Fig. 6.

The change of the orientation angle $\Delta\psi_v^m$ is added to the absolute angle ψ_v^m between the longitudinal axes of the vehicle and the map coordinate system. The vehicle is turning relative to the map. This is an important advantage as the map is only shifted in x^m and y^m -direction. Thus discretization errors, which would occur, if the map would be turned relative to the vehicle, are eliminated. Fig. 7 shows an example.

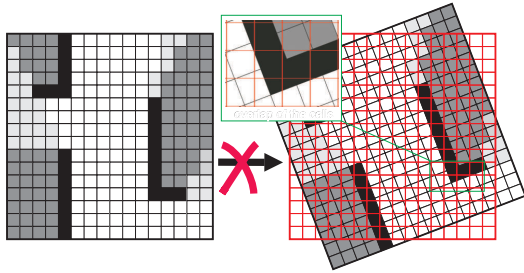


Fig. 7. If the map is rotated relative to the vehicle’s coordinate system, discretization errors in the overlapping regions would occur. That’s why the vehicle is rotated relative to the map coordinate system.

If there are any temporal errors concerning the laser scanner or the ego motion estimation, the online map will be up to date in a very short time, after sensors work reliable again. This is an important fact for the development of robust applications based on the online map.

IV. LANE DETECTION USING THE ONLINE MAP

Much work has been done in the field of detecting lanes and lane markings using video cameras [7]. Also approaches

for the detection and estimation of lane boardings and lane markings using laser scanners were proposed [8], [9].

Most of the laser scanner based approaches are based on model assumptions and significant features, such as a clothoid shape and detected reflexion posts. These approaches work well in highway scenarios, where significant features, such as reflexion posts, crash barriers or lane markings, can be found. However, in urban scenarios, the estimation of the driving path is more challenging, as there are no common features such as reflexion posts etc. Furthermore, the driving path is often reduced by parking cars or other obstacles. Lane markings are often occluded, not visible or even not present in urban scenarios. Therefore, objects at the road boundary form the driving corridor.

The road boundaries are detected and the position of the host vehicle within the driving path is determined using the online map in order to provide these informations to driver assistant and safety systems.

A. Detection of the driving path and lane boundaries

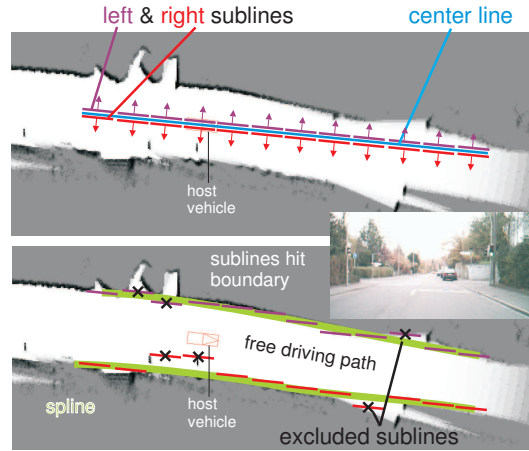


Fig. 8. Principle of the road corridor detection algorithm (urban scenario). Sub lines expand perpendicular from a center line until a border is reached.

Stationary objects, which form the boundaries of the valid driving path, are registered in the online map. Fig. 8 illustrates the principle of a new road corridor detection algorithm. The algorithm performs in the following steps:

- 1) Firstly, a *center line* is determined, which points in the direction of the host vehicle’s longitudinal axis as shown in Fig 8. The line has a maximum length l_{max} . If the line hits a boundary, the line is shortened and it points from the vehicle to the boundary.
- 2) The line is partitioned into several sub lines.
- 3) Each sub line moves perpendicular from the center line until occupied cells in the online map are reached. This is performed for both sides of the center line. If no boundary is found for a sub line in the lateral position of the vehicle, the sub line will be neglected.
- 4) The center of each sub line is calculated.
- 5) An iterative optimization algorithm choses sub lines, which form the road corridor:

- Valid sub lines must be situated on a parabolic curve in order to detect outliers.
- The left and right parabolic curve must have a similar distance to each other.

Further examples from urban and highway scenarios are shown in Fig. 9.

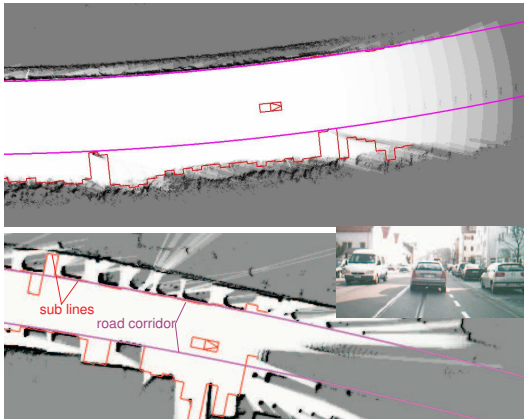


Fig. 9. *Upper Image:* Determination of the road corridor (magenta line) in a highway scenario. The curvature of the road corridor and the lateral distance of the vehicle are determined with the help of the red sub lines. *Lower Image:* Determination of the road corridor in an urban scenario.

This algorithm works well in standard straight or curved road scenarios. However, at intersections and turnoffs, there is more than one possible driving path. Therefore, the algorithm was extended by the following steps:

- 1) The raw shapes of the free regions in the online map are determined.
- 2) *Two center lines* are defined for the intersection as illustrated in Fig. 10.
- 3) Sub lines are used to detect the boundary of the intersection.

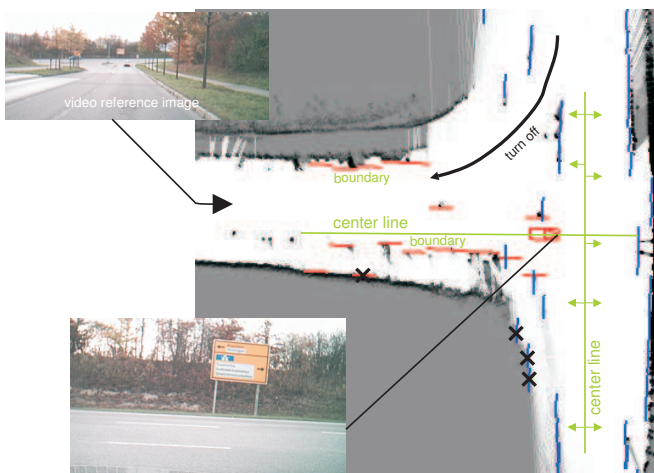


Fig. 10. Road boundary detection in an exemplary intersection scenario.

In the last step the lateral distance between the vehicle and the boundary is calculated. Also the orientation and the position of the vehicle relative to the road is determined.

Fig. 11 shows the result of a lane change maneuver on a highway scenario.

The question may arise, that the lateral offset could also be estimated using video processing. However, the proposed approach will also work in bad visual conditions and if there are no lines on the road and furthermore in urban areas.

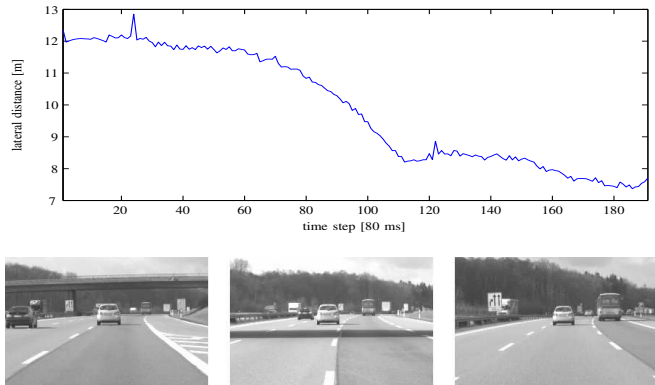


Fig. 11. Lane changing maneuver on a highway. The lateral distance over time is plotted.

V. DETECTION OF MOVING OBJECTS USING ONLINE MAPS

Although the proposed algorithm works well in many scenarios there's one drawback, which is considered for in this section. Distance measurements of the backs of objects moving in front of the host vehicle are registered in the online map. However, the cells are cleared after some scans, but the effect leads to a trail in the online map. These trails are disadvantageous for the road corridor detection algorithm introduced in the last section.

However, these trails are unique features for moving objects. Thus, the detection of trails allows for a robust detection of moving objects independent of their shape and their velocity. Fig. 12 shows some exemplary trails of cars and of a truck in urban and highway scenarios. The likelihoods in the region of moving objects in the online map are shown in a 3D plot.

In order to find trail candidates, lines pointing in parallel direction relative to the laser scanner are defined. Along these lines the likelihoods of passed cells are analyzed. The typical trail shape as shown in Fig. 12 is searched for.

After the detection of a trail, the driving direction of the moving object is determined. The driving direction is perpendicular to the peaks in the online map (see Fig. 12). After the determination of the driving directions the means of the peaks are calculated. Furthermore, the velocity \bar{v}_{obj} of a moving object is calculated by analyzing the average distances of the peaks \bar{d} under consideration of the scan frequency f_{scan} :

$$\bar{v}_{obj} = \bar{d} \cdot f_{scan} \tag{10}$$

Extensive tests have shown, that this trail is observed by all moving vehicles, such as buses, trucks and cars. For bikes the trail is more narrow, but the algorithm also works for these

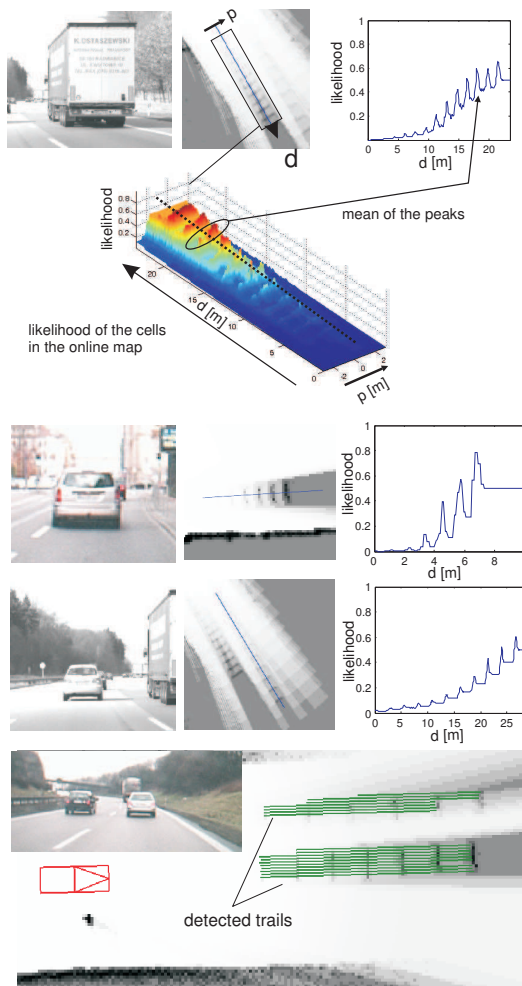


Fig. 12. Moving objects are detected in the online map. Therefore trail shapes are searched for. The width p and the length d of the trails are determined. A 3D shape visualizes the likelihood of cells, where a trail was detected. The peaks are detected and the means of the peaks are calculated. The results are the right plots. The velocity of the moving objects is determined. Lower image: Detected trails of two cars driving in front of the testing vehicle. The green lines show the positions in the online map, where trails can be found. The sub line algorithms exclude these regions for a more robust road corridor detection.

objects. The analysis of the trails is reasonable for objects moving at a relative angle of up to $\pm 90^\circ$ degree relative to the host vehicle in regions, which have not been observed before by the laser scanner. Consequently, the velocity of proceeding objects is calculated without using a common multi-object tracking approach.

The accuracy of the velocity determination using the online map was analyzed. Therefore, the velocity of a reference vehicle was determined precisely using the integrated wheel speed encoders. The testing vehicle followed the reference vehicle and determined its velocity using the online map. The accuracy of the velocity determination is in the region of 1 – 2 km/h. Fig. 13 shows the results.

Moving objects are excluded from the online map, in order to improve the detection of the road corridor. Vehicles driving towards or across the host vehicle are not registered in the online map, because they pass free regions with low

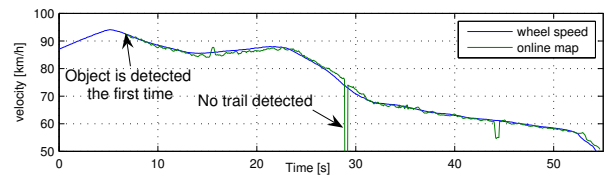


Fig. 13. Velocity of the reference vehicle and the velocity determined from the online map of the testing vehicle driving behind the reference vehicle.

likelihood of occupancy. The trail detection algorithm can be used for various applications. The robust algorithm is applicable in real-time.

VI. CONCLUSIONS AND FUTURE WORKS

A. Conclusions and Future Works

An algorithm for the real time generation of an online map based on binary bayes filter and laser scanner data is proposed. A robust algorithm for the detection of the driving corridor in urban and highway scenarios is introduced. Furthermore, an algorithm for the detection of moving objects using the online map is proposed.

VII. ACKNOWLEDGMENTS

This work is supported by IBEO Automobile Sensor GmbH (www.ibeo-as.de). Further information is available on www.argos.uni-ulm.de

REFERENCES

- [1] N. Kaempchen, M. Buehler, and K. Dietmayer, "Feature-level fusion for free-form object tracking using laserscanner and video," *Proceedings of 2005 IEEE Intelligent Vehicles Symposium, Las Vegas, USA*, 2005.
- [2] S. Wender, T. Weiss, K. Fuerstenberg, and K. Dietmayer, "feature level fusion for object classification", in *PreVENT ProFusion e-Journal, Vol. 1, 2006*, 2006.
- [3] S. Thrun, D. Fox, and W. Burgard, *Probabilistic Robotics*. MIT Press, 2005.
- [4] S. Thrun, "Learning occupancy grid maps with forward sensor models." [Online]. Available: citeseer.ist.psu.edu/701378.html
- [5] S. et. al. Thrun, S. et. al. Strohsand, and G. et. al. Bradski, "Stanley: The robot that won the darpa grand challenge," *Journal of Field Robotics 23(9)*, Wiley Periodicals, Inc., p. 661–692, 2006. [Online]. Available: www.interscience.wiley.com
- [6] Website: *IBEO Automobile Sensor GmbH*. IBEO, 2006. [Online]. Available: www.ibeo.de
- [7] M. S. von Trzebiatowski, A. Gern, U. Franke, U.-P. Kaeppler, and P. Levi, "Detecting reflection posts - lane recognition on country roads," in *2004 IEEE Intelligent Vehicles Symposium, University of Parma, Parma, Italy*, 2004.
- [8] A. Kirchner, *Sensordatenverarbeitung eines Laserscanners fuer autonome Fahrfunktionen von Kraftfahrzeugen - Sensor data processing for laser scanners for autonomous driving applications*. Universitt der Bundeswehr, PhD Thesis, 2000.
- [9] K. Dietmayer, N. Kaempchen, and K. Fuerstenberg, "Roadway detection and lane detection using multilayer laserscanner," in *Proceedings of Advanced Microsystems for Automotive Applications 2005*, 2005.